Modeling and Analysis of Cushioning Performance for Multi-layered Corrugated Structures

Jong Min Park[1]*, Ghi Seok Kim[2], Soon Hong Kwon[1], Sung Won Chung[1], Soon Goo Kwon[1], Won Sik Choi[1], Jong Soon Kim[1]

[1]*Department of Bioindustrial Machinery Engineering, Pusan National University, Korea*
[2]*Department of Biosystems and Biomaterials Engineering, Seoul National University, Korea*

Abstract

Purpose: The objective of this study was to develop cushion curves models and analyze the cushioning performance of multi-layered corrugated structures (MLCS) using a method based on dynamic stress-energy relationship. **Methods:** Cushion tests were performed for developing cushion curve models under 12 combinations of test conditions: three different combinations of drop height, material thickness, and static stress for each of four levels of energy densities between 15 and 60 kJ/m^3. **Results:** Dynamic stress and energy density for MLCS followed an exponential relationship. Cushion curve models were developed as a function of drop height, material thickness, and static stress for different paperboards and flute types. Generally, the differences between the shock pulse (transmitted peak acceleration) and cushion curve (position and width of belly portion) for the first drop and the averaged second to fifth drop were greater than those for polymer-based cushioning materials. Accordingly, the loss of cushioning performance of MLCS was estimated to be greater than that of polymer-based cushioning materials with the increasing number of drops. The position of the belly of the cushion curve of MLCS tends to shift upward to the left with increasing drop height, and the belly portion became narrower. However, depending on material thickness, under identical conditions, the cushion curve of MLCS showed an opposite tendency. **Conclusions:** The results of this study can be useful for environment-friendly and optimal packaging design as shock and vibrations are the key factors in cushioning packaging design.

Keywords: Cushion curve, Cushioning packaging design, Dynamic stress-energy method, Multi-layered corrugated structure, Shock pulse

Introduction

Packages experience mechanical stresses such as shocks and vibrations during transport and distribution. The destructive effects of these physical stresses can generally be reduced by using cushioning materials to improve the protection of fragile goods during distribution (Park and Han, 2011; MIL-HDBK-304C). Because of the negative environmental impact of using traditional polymeric cushioning materials for cushioning in transport packaging design, optimum cushioning packaging design

replacing or reducing the amount of cushioning materials has gained interest in recent years.

The shock absorbing performances of cushioning materials are presented through cushion curves, which are graphs of the peak acceleration of shocks versus the corresponding static stress, presented over a range of static stress conditions for a specific material thickness and a specific drop height (Park and Han, 2011; MIL-HDBK-304C). The cushion curves are mainly used to design and optimize cushion packaging. These curves make it possible to determine the minimum thickness, the bearing area of the cushion, and the required static stress, which are all essential in cushioning packaging design.

The traditional method to obtain the cushion curves of

*Corresponding author: Jong Min Park
Tel: +82-55-350-5424; **Fax:** +82-55-350-5429
E-mail: parkjssy@pusan.ac.kr

a specific material is described in ASTM D 1596, but this method requires enormous amounts of test data: data of a series of impacts for a range of static stresses, drop heights, and material thickness, involving many replications. Therefore, this method is time consuming and cost intensive.

In recent years, alternative methods were developed to obtain cushion curves in a significantly shorter time for testing (Burgess, 1990; 1994; Sek et al., 1997; 2000). Representatives of alternative methods are the dynamic stress-energy method (Burgess, 1990; 1994) and the single compression data method based on a quasidynamic compression test (Sek et al., 1997; 2000).

In the dynamic stress-energy method, the cushion curve is modeled on the basis of dynamic stress and energy density obtained independently. A dynamic stress-energy density curve is drawn using peak accelerations obtained from few cushion tests; thereafter, a cushion curve model is created with the variables static stress, material thickness, and drop height through a regression analysis of the curve. The single compression data method is a technique of obtaining a family of cushion curves by using a dynamic factor calculated from the relation between the compression behaviors obtained from each condition of quasidynamic compression and shock.

Singh et al. (2010) reported that the dynamic stress-energy method can greatly save time in predicting the transmitted shock for calculating cushion curves of closed cell foams. However, this method has an error of more than 5% when compared to the test results of ASTM D 1596. Patricia Navarro-Javierre et al. (2012) compared the cushion curves of closed cell foams (polyethylene Ethafoam and expanded polystyrene) obtained by both the dynamic stress-energy method and single compression data method with those calculated by ASTM D 1596 method. They showed that the difference between cushion curves obtained by the single compression data method (compression strain rate, 0.425 m/s) and ASTM D 1596 was small—up to 75 cm of drop height: 0.425 m/s of compression strain rate is equal to 11% of the impact velocity from a drop height of 75 cm. However, the difference was greater for drop height greater than 75 cm. Further, to reduce the error, they also suggested an improvement method that involved increasing the compression strain and compression strain rate and the application of a dynamic factor. They also showed that differences appeared between the cushion curves obtained by the dynamic stress-energy
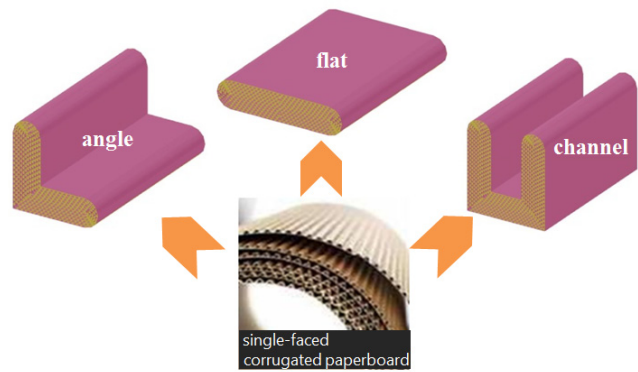

Figure 1. Various types of multi-layered corrugated structure.

method and ASTM D 1596 at both ends of the applied static stress range and that the difference increased with increasing drop height.

Campbell (2010) used a dynamic stress-energy method to calculate the cushion curve of single-wall (SW) corrugated paperboard (A/F, B/F) and double-wall (DW) corrugated paperboard (AC/F, BC/F). Marcondes (2010) employed the method to determine the minimum sample size for calculating the cushion curve of closed-cell foam, and he reported three energy levels for the minimum sample size. Potter (2010) also applied this method to estimate the cushion performance of expanded polymer cushioning materials, which are less than one inch thick.

Multi-layered corrugated structures (MLCS) are made by laminating numerous single-faced corrugated paperboards, and this is a typical environment-friendly cushioning material with little environmental impact. In such packaging, the energy absorbing characteristics of flute are employed for protection against shocks and vibrations (Kim et al., 2013). As shown in Figure 1, various types of MLCS packaging—edge pads (for angles), side pads (for channels), and face pads (for flat surfaces)—can be produced to suit the shapes of the products to be packaged.

Cushioning performance of polymeric cushioning materials is sensitive to service temperature (Marcondes et al., 2003), while that of cellulose-based cushioning materials such as MLCS tends to change with relative humidity (Marcondes, 1992).

Cushioning performance, vibration transmissibility, and compressive resistance of MLCS were examined in detail in previous works (Wang, 2009; Guo et al., 2011; Kim et al., 2013; Wang et al., 2013). Guo et al. (2010) considered the shape of the shock pulse of the MLCS as a half-sine wave, and they approximated the cushion curve of the peak acceleration-static stress with a third-degree poly-

nominal. They also reported that a drop height is a significant variable for dynamic cushioning performance because the position of the belly on the cushion curve shifts upward to the left with increasing drop height, while for identical drop heights, the belly shifts downward with increasing the number of layers of the MLCS. Guo et al. (2011) approximated the cushion curve of X-PLY MLCS with a quadratic polynomial, and showed that the dynamic cushioning performance of X-PLY with A/F is better than that of X-PLY with B/F because the position of the belly on the cushion curve of the former is lower than that of the latter under identical drop height conditions. On the other hand, Guo and Zhang (2004) approximated the cushion curve of honeycomb paperboards with a sandwich structure, such as corrugated paperboard, with a third-degree polynomial, and reported that the position of the belly on the cushion curve shifted upward with increasing drop height shifted downward to the right with increasing material thickness under identical drop height conditions. Marcondes (1992) analyzed the effect of relative humidity on the cushion curves of SW and DW corrugated paperboards, and Campbell (2010) analyzed the changes in the resilience and cushion performance of SW and DW corrugated paperboards according to the number of drops.

As shown above, domestic studies on MLCS as cushioning packaging material are lacking, and the results of studies overseas have limited applications to cushioning packaging design because of the limitations imposed by the specific properties of materials and test conditions.

The objectives of this study were to analyze the cushioning performance of the MLCS that are commonly used in South Korea for different paperboards and flute types by using the dynamic stress-energy method, and to develop their cushion curve models.

Materials and Methods

Experimental design

In the experimental design for calculating the cushion curve using the dynamic stress-energy method, the independent variables are drop height, material thickness, and static stress, and the dependent variable is peak acceleration (Daum, 2006; Park and Han, 2011). Therefore, the energy density level containing all of the independent variables should be determined first.

Energy density was classified into four levels, namely, 15, 30, 45, and 60 kJ/m^3 by considering the characteristics of MLCS determined through a preliminary test and the specifications of the cushion tester. For each energy density level, three combinations of independent variables were considered, as presented in Table 1.

Experimental apparatus and method

Figure 2 shows the free-fall type cushion tester used in this study. The schematic and block diagram of the system are shown in Figure 3.

Free fall is realized by operating an electromagnet. The impact energy of the tester can be determined by changing the dummy weight and drop height (maximum 1.6 m). In order to realize perfect face contact between the drop apparatus (comprising a guided platen, a dummy weight,

Table 1. Experimental design for deriving cushion curves of *MLCS* by dynamic stress vs. energy method

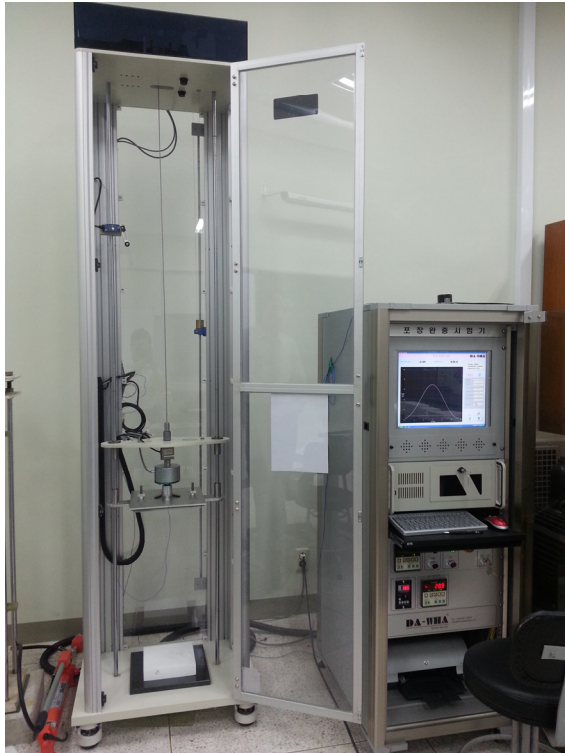| Drop #	Energy density $DE = \sigma_{st} \times h/t$ (kJ/m^3)	Drop height h (cm)	Weight W (kgf)	Static stress σ_{st} (kPa)	Sample size $\ell \times w \times t$ (cm)
15-1		48.5	5	0.927	23 × 23 × 3
15-2	15	13.8	5	2.180	15 × 15 × 2
15-3		25.1	11	2.989	19 × 19 × 5
30-1		64.7	5	0.927	23 × 23 × 2
30-2	30	34.4	6	2.616	15 × 15 × 3
30-3		46.0	12	3.261	19 × 19 × 5
45-1		47.3	7	1.902	19 × 19 × 2
45-2	45	34.4	6	2.616	15 × 15 × 2
45-3		59.0	7	3.052	15 × 15 × 4
60-1		63.1	7	1.902	19 × 19 × 2
60-2	60	73.6	9	2.446	19 × 19 × 3
60-3		78.6	7	3.052	15 × 15 × 4

Figure 2. Experimental apparatus for cushion testing.

(1) accelerometer
(2) electromagnet
(3) guide shaft
(4) dummy weight
(5) ball bush
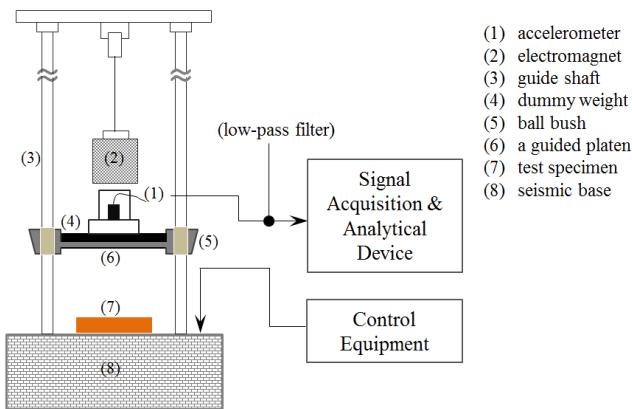(6) a guided platen
(7) test specimen
(8) seismic base

Figure 3. Schematic of the cushion testing setup.

and an accelerometer) and the specimen during impact, cylindrical ball bushes are installed at the joints between the drop apparatus and guide shafts. Because the loss of impact energy due to friction between the guided platen and guide shaft was minimized, the equivalent free-fall drop height determined by actual measurement of the drop apparatus velocity was not implemented separately.

A piezoelectric type accelerometer (352A25, PCB Piezotronics, Inc., USA) with a flexible cable was used in the cushion tester. Its measurement range, sensitivity, and frequency response are 2000 G (maximum), 2.5 mV/G,
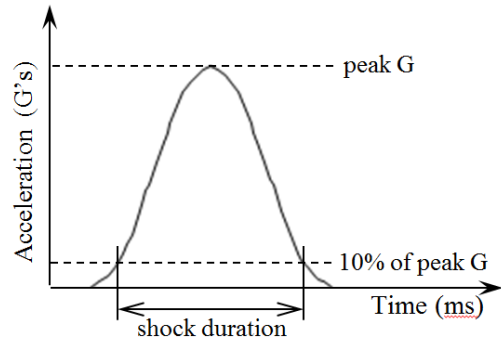

Figure 4. Illustration of the effective shock pulse duration.

and 10 kHz (maximum), respectively. The accelerometer, which is rigidly installed on the guided platen, measures the acceleration transmitted through the test specimen during an impact.

High-frequency noise with vibration signals due to the mechanical equipment was eliminated by employing an electron filter system to avoid distortion of the shock pulse, and the bandwidth of the cutoff frequency was calculated by using Equation (1) (Marcondes, 2010). That is, frequencies higher than five times both the natural frequency ($f_n=1/2\tau$) of shock pulse and the shock pulse itself were eliminated by the low-pass filter.

$$f_f \geq 10\left(\frac{1}{2\tau}\right) \tag{1}$$

where f_f is the filtering frequency (Hz), and τ is the shock duration (ms).

The shock duration used in Equation (1) was determined as the full width at 10% of the peak acceleration, as shown in Figure 4 (MIL-HDBK-304C).

The test specimens were kept in a constant temperature and humidity chamber (22°C, relative humidity 50%) for 72 h before the test. Drop tests were performed five times for each specimen, and the testing results were divided into those for the first drop and those averaged for the second to the fifth drops (ASTM D 1596). The experiment was conducted in triplicate for each test condition, as presented in Table 1, and the average value was obtained.

Materials

Test samples used in the analysis of cushioning performance of MLCS were classified as A/F and B/F with regard to the flute and S120 and K180 with regard to the

Table 2.	Specifications of the *MLCS* used for the cushion testing	
Paperboards[a]	Flute type	Specifications
S120	A/F	· height, wave length, and take-up-factor of the flute:
	B/F	4.6 mm, 8.8 mm, and 1.6, respectively, for *A/F*; 2.6 mm, 6.0 mm, and 1.4, respectively, for *B/F*
K180	A/F	· thickness of paperboard: 0.24 mm (*K180*); 0.19 mm (*S120*)
	B/F	· ring crush[b]: 198 N (*K180*); 82 N (*S120*)

[a]*S120* and *K180*; Korean old corrugated container (KOCC) (100)
[b]KS M ISO 12192

Table 3.	The number of layers of single-faced corrugated paperboard and total basis weight according to nominal thickness of the *MLCS* used for the cushion testing												
		Nominal thickness, *t*											
Paperboards	Flute type	20 mm			30 mm			40 mm			50 mm		
		t_a[a]	layers[b]	*TBW*[c]	t_a	layers	*TBW*	t_a	layers	*TBW*	t_a	layers	*TBW*
S120	A/F	17.0 (±0.32)	4	1248	27.5 (±0.31)	6	1872	37.0 (±0.41)	8	2496	48.3 (±0.44)	10	3120
	B/F	19.1 (±0.24)	6	1728	29.5 (±0.27)	9	2592	39.3 (±0.27)	12	3456	49.7 (±0.38)	15	4320
K180	A/F	18.8 (±0.33)	4	1872	28.1 (±0.28)	6	2808	37.7 (±0.38)	8	3744	48.7 (±0.43)	10	4680
	B/F	20.0 (±0.21)	6	2592	29.6 (±0.25)	9	3888	39.2 (±0.23)	12	5184	48.6 (±0.30)	15	6480

[a]All data (actual thickness measured) represent the mean of 10 determinations
[b]The number of layers of single-faced corrugated paperboard
[c]Total basis weight of *MLCS* (gf/m^2), $TBW = BW_{sf} \times n = (BW_\ell + BW_f \times t_f) \times n$
(BW_{sf} = basis weight of single-faced corrugated paperboard; n = the number of layers of single-faced corrugated paperboard; BW_ℓ and BW_f = basis weights of the liner and corrugating medium, respectively; and t_f = take-up-factor of flute)

paperboard. The actual thickness of the sample and the number of layers of single-faced corrugated paperboard according to the nominal thickness of the sample are listed in Table 3.

As shown in Figure 5, the samples used in the study were classified into four types based on their nominal thickness—20, 30, 40, and 50 mm. They were further subdivided into subtypes depending on the dimensions

(length × width): 15 × 15 mm, 19 × 19 mm, and 23 × 23 mm for nominal thicknesses of 20 mm and 30 mm; 15 × 15 mm for a nominal thickness of 40 mm; and 19 × 19 mm for a nominal thickness of 50 mm.

Results and Discussion

Modeling for cushion curves

The dynamic stress calculated by using Equation (3) with the peak acceleration of the shock pulse, which was obtained by cushion testing, is presented in Table 4 (Burgess, 1990; 1994).

$$DE = \frac{\sigma_{st} \times h}{t} \tag{2}$$

$$DS = G_p \times \sigma_{st} \tag{3}$$

where *DE* is the energy density (dynamic energy; J/m^3);

Figure 5. Various specimens of the planned dimensions.

Table 4. Values of dynamic stress calculated from these values and the measured peak accelerations

Drop #	DE (kJ/m³)	S120								K180							
		$G_p^{1)}$ (G's)				DS (kPa)				G_p (G's)				DS (kPa)			
		A/F		B/F		A/F		B/F		A/F		B/F		A/F		B/F	
		1st[2)	ave.[3)]	1st	ave.	1st	ave.	1st	ave.	1st	ave.	1st	ave.	1st	ave.	1st	ave.
15-1		51	140	65	108	47	130	60	100	56	96	55	100	52	89	51	93
15-2	15	26	64	32	50	57	140	70	110	27	44	27	46	59	96	58	100
15-3		22	50	27	40	67	150	80	120	22	34	22	36	66	103	65	107
30-1		87	202	70	156	81	187	65	145	56	133	72	147	52	123	67	136
30-2	30	37	77	31	61	96	202	80	160	25	52	31	57	65	136	80	150
30-3		34	66	29	54	111	217	95	175	24	46	29	50	78	150	94	164
45-1		68	137	47	115	130	260	90	218	41	86	45	104	79	165	85	197
45-2	45	57	107	42	91	150	280	110	238	37	70	39	82	97	182	103	215
45-3		56	98	42	85	170	300	130	258	38	65	40	76	115	200	121	233
60-1		94	190	69	155	179	362	132	295	53	124	61	146	101	237	117	277
60-2	60	83	158	64	131	204	387	157	320	51	106	57	123	124	260	140	300
60-3		75	135	60	113	229	412	182	345	48	93	33	106	147	283	163	323

Note: 1) All data represent the mean of 3 determinations. 2) 1st drop, 3) averaged 2nd~5th drop

σ_{st}, static stress (Pa); h, drop height (m); t, material thickness (m); G_p, peak acceleration (Pa); and DS, dynamic stress (Pa).

Figure 6 shows the relation between dynamic stress and energy density for different paperboards and flute types of MLCS. Overall, dynamic stress tends to increase exponentially with increasing energy density, and both the dynamic stress and the increasing rate of the averaged value for the second to fifth drop in the two types of paperboard MLCS were higher than those of the first drop. In addition, there was a large difference between the dynamic stresses by the flute type of MLCS. That is, the results for A/F were higher than those for B/F for the MLCS in S120 (p < 0.01), and the converse was true for the MLCS in K180 (p < 0.01). The difference between the dynamic stress of the two flutes increased with increasing energy density.

Because the behavior of dynamic stress-energy density of MLCS is similar to that of polymeric cushioning materials, the relationship was calculated by nonlinear regression analysis with an exponential form (Burgess, 1990; Daum, 2006; Patricia Navarro-Javierre et al., 2012) using commercial software DataFit (Version 7.1, Oakdale Engineering, USA). The cushion models were then derived from the results (Table 5).

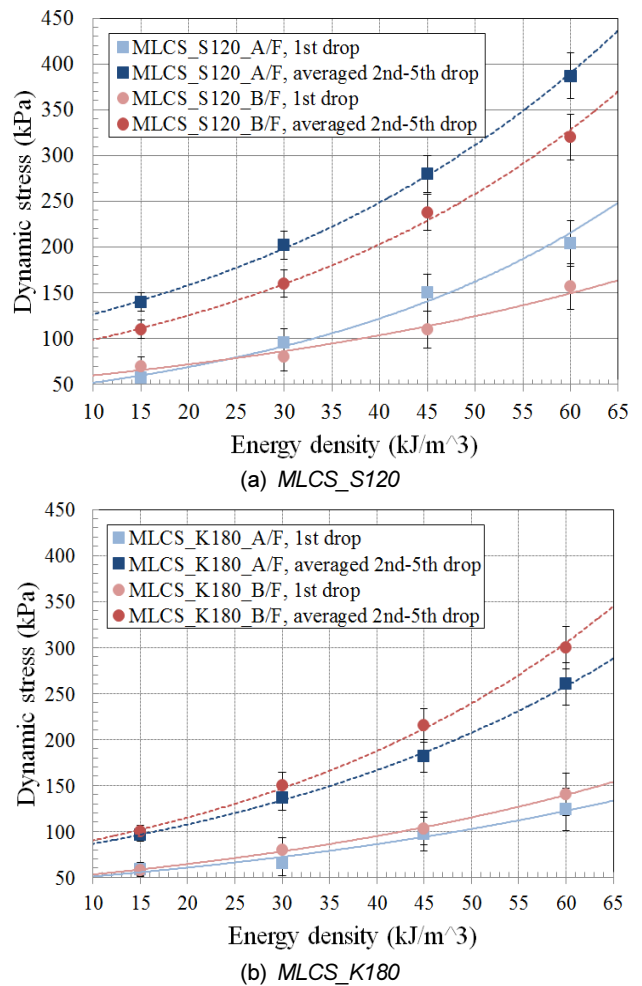$$DS = a \times e^{b(DE)} \rightarrow G_p = a \times e^{b(\sigma_{st} \times h/t)}/\sigma_{st} \qquad (4)$$

(a) *MLCS_S120*

(b) *MLCS_K180*

Figure 6. Relationships between dynamic stress and energy density for MLCS.

Table 5. Results of modeling for cushion curves of *MLCS*

Classification		$G_p = a \times e^{b(\sigma_{st} \times h/t)}/\sigma_{st}$					
		1st drop			Averaged 2nd–5th drops		
		a	b	r^2	a	b	r^2
S120	A/F	43.5659 (0.015)[1]	0.0261 (0.008)	0.99	102.7083 (0.000)	0.0221 (0.000)	0.99
	B/F	46.7856 (0.012)	0.0198 (0.012)	0.99	80.8078 (0.004)	0.0231 (0.003)	0.99
K180	A/F	41.5269 (0.012)	0.0182 (0.015)	0.97	68.8896 (0.001)	0.0220 (0.001)	0.99
	B/F	43.9072 (0.001)	0.0193 (0.001)	0.99	72.8504 (0.001)	0.0237 (0.001)	0.99

Note: 1) Numbers in parenthesis are p values.

From the cushion curve models listed in Table 5, the peak acceleration for different combinations of drop height, material thickness, and static stress can be calculated.

(a) 1st drop

(b) averaged 2nd-5th drop

Figure 7. Examples of cushion curves calculated from cushion curve models (*MLCS_K180_A/F*).

Thus, the cushion curves for specific conditions can be derived.

The conventional cushion curves calculated by ASTM D 1596 provide limited information for specific conditions. However, the modeling of cushion curve by the dynamic stress-energy method presents an opportunity to obtain a large amount of data (Burgess, 1990; Daum, 2006; Park and Han, 2011). Representative cushion curves calculated from the cushion curve models listed in Table 5 are shown in Figure 7.
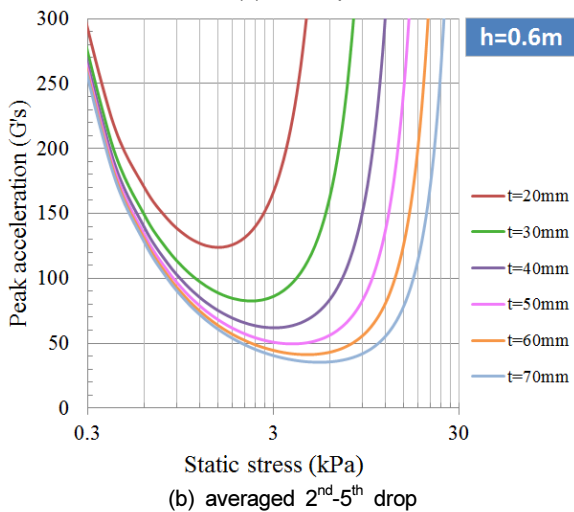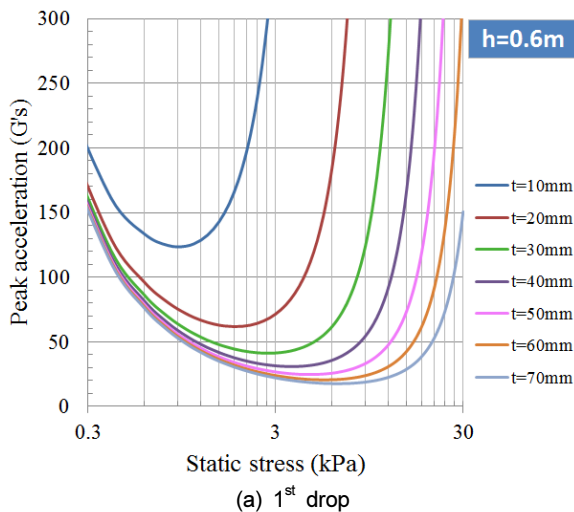
Shock pulse according to the flute type and paperboards

In case of the polymeric cushioning materials, the transmitted peak acceleration tends to increase with increasing number of drops. Therefore, when deriving cushion curve by ASTM D 1596, the results for the first drop and those for the averaged second to fifth drop are considered, and these two curves represent one set.

However, in the case of the MLCS, it was observed that the transmitted peak acceleration remained constant or decreased until the second or third drop at low levels of energy density (the low levels of drop height and static stress). However, it rapidly increased with the number of drops owing to the decrease in flute resilience. These results are attributed to the softening characteristics of MLCS and are significantly different from those of polymeric cushioning materials. This outcome is similar to the previous research result for SW corrugated paperboard reported by Campbell (2010). However, the transmitted peak accelerations of the averaged second to fifth drops were much greater than those of the first drop for the MLCS used in the study. The difference between these

values was greater than that for polymeric cushioning materials under identical test conditions. On the basis of these results, the loss of cushioning performance of MLCS cushioning materials is considered greater than that of polymeric cushioning materials with increasing number of drops.

However, different results were observed for high levels of energy density (the high levels for the drop height and static stress). This observation can be explained using the expression, $G_p = \sqrt{2kh/W}$ relating the elastic modulus and transmitted acceleration of material. That is, the acceleration transmitted through the material is proportional to the square root of the elastic modulus of material, which is always related to the weight of the object (Park and Han, 2011; Marcondes, 1992).

In case the MLCS in S120, the transmitted peak acceleration of B/F was higher than that of A/F for the first drop, and the transmitted peak acceleration of A/F was higher than that of B/F for the averaged second to fifth drop. On the other hand, in the case of the MLCS in K180, the transmitted peak acceleration did not differ between two flutes for the first drop, but for the averaged second to fifth drops, the transmitted peak acceleration of B/F was higher than that of A/F.

There is no difference between the transmitted peak accelerations of the MLCS in two paperboards under the low level of energy density, but the transmitted peak acceleration of the MLCS in S120 was greater than that of the MLCS in K180 with increasing energy density for all flute types. This phenomenon is attributed to the sharp loss of resilience by rapid crushing of the flute of the MLCS in S120 (Table 4).

Cushioning characteristics

As shown in Figure 7, the cushion curve of MLCS has a downward convex shape with a minimum knee point (i.e., belly) (Marcondes, 1992; Guo and Zhang, 2004; Campbell, 2010; Guo et al., 2010; 2011).

At the left side of the belly on the cushion curve, because of the low masses of the weight and drop block, the drop shock causes very little compressive deformation. Therefore, the absorbing energy (strain energy) per unit volume of the cushioning material is reduced, resulting in large transmitted acceleration. On the other hand, at the right side of the belly, the masses of the weight and drop block are great, leading to severe compression of the corrugated paperboard. As a result, the corrugated paperboard is bottomed out. Thus, the minimum peak acceleration increases. However, because the compressed condition of the cushioning material at the belly of the cushion curve is satisfactory, the absorbing energy per unit volume of materials is large, and the transmitted acceleration is small. Therefore, because the cushioning material exhibits optimal cushioning performance at the belly of its cushion curve, such a condition is applied in cushioning design. That is, when the left and right parts from the belly of the cushion curve are applied for cushioning design, under-packaging (under-bearing area for cushioning) and over-
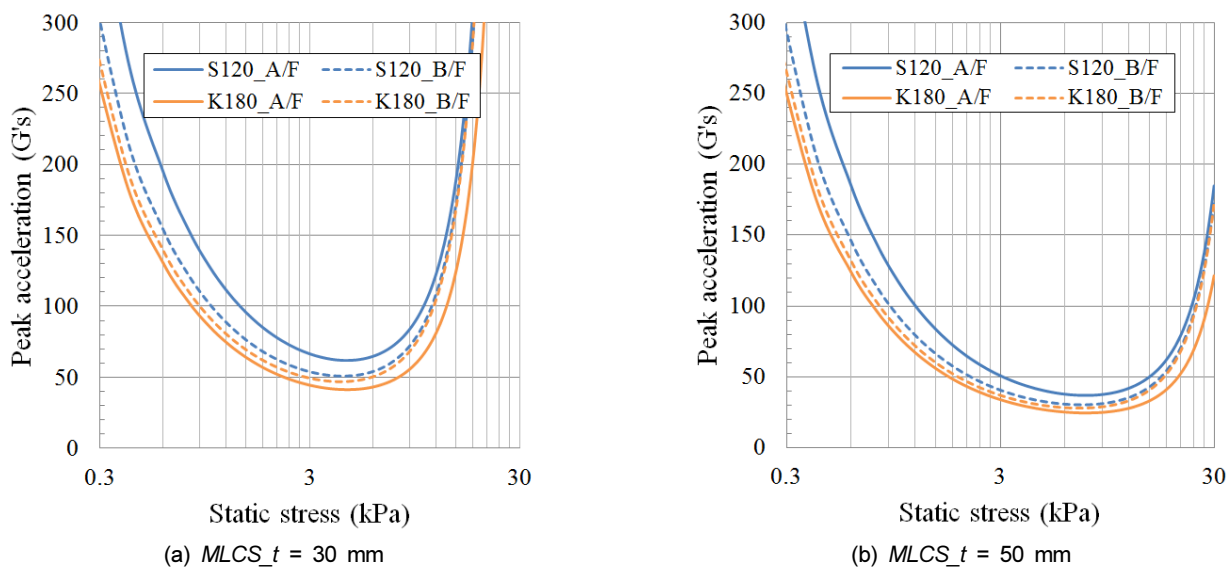

(a) *MLCS_t* = 30 mm

(b) *MLCS_t* = 50 mm

Figure 8. Cushion curves of MLCS as a function of paperboards and flute types at a drop height of 30 cm (averaged second to fifth drops).
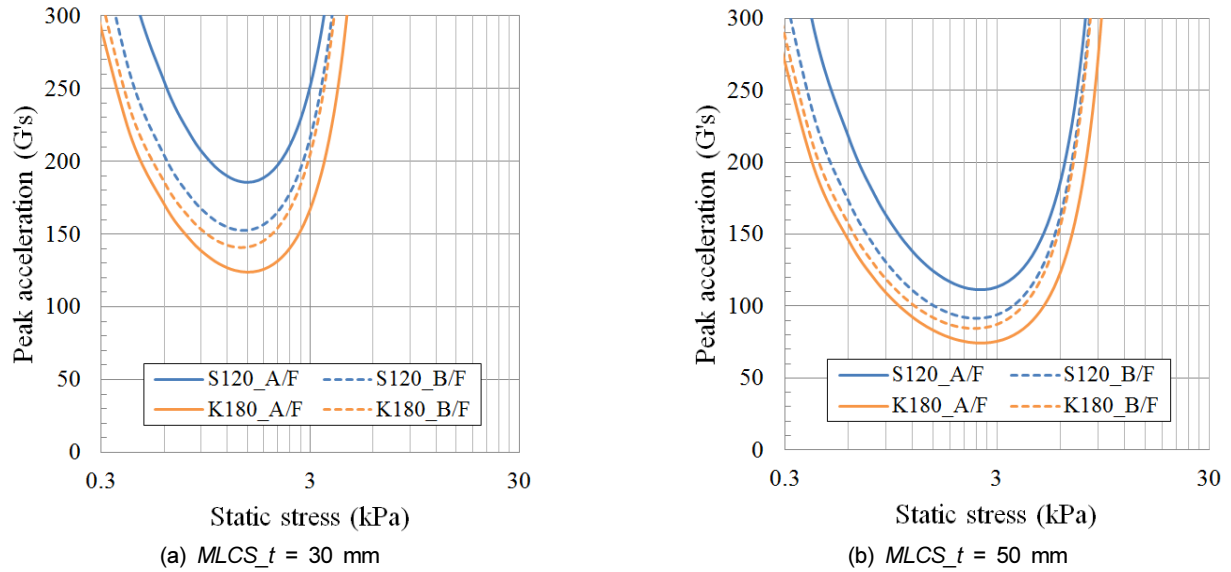
(a) MLCS_t = 30 mm

(b) MLCS_t = 50 mm

Figure 9. Cushion curves of MLCS as a function of paperboards and flute types at a drop height of 90 cm (averaged second to fifth drops).

Table 6. Position of the belly (G_p, σ_{st}) (G's, kPa) on the cushion curve according to paperboards, flute type, material thickness, and drop height

Classify		t (mm)	1st drop				Averaged 2nd~5th drops			
			Drop height (cm)				Drop height (cm)			
			30	60	90	120	30	60	90	120
S120	A/F	20	(46,2.6)	(93,1.2)	(139,0.8)	(186,0.6)	(93,3.0)	(186,1.6)	(278,1.0)	(372,0.8)
		30	(31,3.8)	(62,2.0)	(93,1.2)	(124,1.0)	(62,4.6)	(124,2.2)	(186,1.6)	(248,1.2)
		40	(23,5.2)	(46,2.6)	(70,1.8)	(93,1.2)	(46,6.0)	(93,3.0)	(139,2.0)	(186,1.6)
		50	(19,6.4)	(37,3.2)	(56,2.2)	(74,1.6)	(37,7.6)	(74,3.8)	(111,2.6)	(149,1.8)
		60	(15,7.6)	(31,3.8)	(46,2.6)	(62,2.0)	(31,9.0)	(62,4.6)	(93,3.0)	(124,2.2)
		70	(13,9.0)	(27,4.4)	(40,3.0)	(53,2.2)	(27,10.6)	(53,5.2)	(80,3.6)	(106,2.6)
	B/F	20	(38,3.4)	(76,1.6)	(114,1.2)	(152,0.8)	(76,2.8)	(153,1.4)	(229,1.0)	(307,0.8)
		30	(25,5.0)	(51,2.6)	(76,1.6)	(101,1.2)	(51,4.4)	(102,2.2)	(153,1.4)	(204,1.0)
		40	(19,6.8)	(38,3.4)	(57,2.2)	(76,1.6)	(38,5.8)	(76,2.8)	(115,2.0)	(153,1.4)
		50	(15,8.4)	(30,4.2)	(45,2.8)	(61,2.2)	(31,7.2)	(61,3.6)	(92,2.4)	(122,1.8)
		60	(13,10.0)	(25,5.0)	(38,3.4)	(51,2.6)	(25,8.6)	(51,4.4)	(76,2.8)	(102,2.2)
		70	(11,11.8)	(22,5.8)	(33,4.0)	(43,3.0)	(22,10.0)	(44,5.0)	(65,3.4)	(87,2.6)
K180	A/F	20	(31,3.6)	(62,1.8)	(93,1.2)	(124,1.0)	(62,3.0)	(124,1.6)	(186,1.0)	(248,0.8)
		30	(21,5.4)	(41,2.8)	(62,1.8)	(82,1.4)	(41,4.6)	(83,2.2)	(124,1.6)	(165,1.2)
		40	(15,7.4)	(31,3.6)	(46,2.4)	(62,1.8)	(31,6.0)	(62,3.0)	(93,2.0)	(124,1.6)
		50	(12,9.2)	(25,4.6)	(37,3.0)	(49,2.2)	(25,7.6)	(50,3.8)	(74,2.6)	(99,1.8)
		60	(10,11.0)	(21,5.4)	(31,3.6)	(41,2.8)	(21,9.0)	(41,4.6)	(62,3.0)	(83,2.2)
		70	(9,12.8)	(18,6.4)	(27,4.2)	(35,3.2)	(18,10.6)	(35,5.2)	(53,3.6)	(71,2.6)
	B/F	20	(35,3.4)	(69,1.8)	(104,1.2)	(138,0.8)	(70,2.8)	(141,1.4)	(212,1.0)	(284,0.8)
		30	(23,5.4)	(46,2.6)	(69,1.8)	(92,1.2)	(47,4.2)	(94,2.2)	(141,1.4)	(188,1.0)
		40	(17,7.0)	(35,3.4)	(52,2.4)	(69,1.8)	(35,5.6)	(70,2.8)	(106,1.8)	(141,1.4)
		50	(14,8.6)	(28,4.4)	(41,2.8)	(55,2.2)	(28,7.0)	(56,3.6)	(85,2.4)	(113,1.8)
		60	(12,10.4)	(23,5.2)	(35,3.4)	(46,2.6)	(24,8.4)	(47,4.2)	(70,2.8)	(94,2.2)
		70	(10,12.0)	(20,6.0)	(30,4.0)	(39,3.0)	(20,9.8)	(40,5.0)	(60,3.2)	(81,2.4)

packaging (over-bearing area for cushioning) of product, respectively, may occur. However, when the belly is applied for cushioning design, an optimal cushioning design can be realized.

In general, the allowable stress increases as the belly moves downward to the right on its cushion curve under identical conditions. Thus, an economical cushioning condition is obtained owing to the decrease in the cushioning area required. In addition, the wider the belly, the larger is the range of applications of the cushioning material owing to the broad range of allowable static stress (MIL-HDBK-304C).

Figures 8 and 9 show the cushion curves of MLCS under specific conditions of drop heights of 30 cm and 90 cm and material thicknesses of 30 mm and 50 mm for different paperboards and flute types. The position of the belly of the cushion curve tends to shift upward to the left with increasing drop height, and the width of the belly decreases. Accordingly, because the drop height is a very important factor in the dynamic cushioning characteristics of a material, the design drop height of the product should correspond to the test drop height when selecting the cushion curve for the cushioning design of a product (Guo et al., 2010).

In addition, the position of the belly of the cushion curve tends to shift downward to the right with increasing material thickness under identical drop height conditions (Guo and Zhang, 2004), and the belly portion becomes wider. The position of the belly for the averaged second to fifth drops was located higher and to the left of that for the first drop, and the width of belly portion decreased. This trend becomes more distinct with increasing drop height.

with drop height, material thickness, and static stress as variables for different paperboards and flute types. In the case of the MLCS, the transmitted peak acceleration remained constant or decreased until the second or third drop. However, the transmitted peak accelerations of the averaged second to fifth drops were much greater than those of the first drop. The difference between these values was greater than those of polymeric cushioning materials under identical test conditions. The position of the belly of the cushion curve of MLCS tends to shift upward to the left with increasing drop height, and the belly portion becomes narrower. In addition, the position of the belly on the cushion curve tends to shift downward to the right with increasing material thickness under identical drop height conditions, and the width of belly increases. The position of the belly for the averaged second to fifth drop was located more to the left and higher than that for the first drop, and the width of the belly decreased. This trend became more distinct with increasing drop height. Generally, the differences between the shock pulse (transmitted peak acceleration) and cushion curve (position and width of the belly) between the first drop and the averaged second to fifth drops was larger than those for polymeric cushioning materials. Accordingly, the loss of cushioning performance of MLCS cushioning material is greater than that of polymeric cushioning materials with an increasing number of drops.

Conflict of Interest

The authors have no financial or other interests.

Conclusion

In this study, the cushioning performance of the MLCS that are commonly used in South Korea was analyzed for different paperboards and flute types by the dynamic stress-energy method. Cushion tests were performed for developing these cushion curve models for 12 combinations of test conditions. Energy density was classified into four levels, namely, 15, 30, 45, and 60 kJ/m^3, and each of the energy density level was sub-classified into three sublevels for combinations of independent variables (drop height, material thickness, and static stress). The dynamic stress and energy density of MLCS exhibited an exponential relationship, and the cushion curve models were developed

Acknowledgement

References

ASTM D 1596:2014. Standard test method for dynamic shock cushioning characteristics of packaging material.

Burgess, G. 1990. Consolidation of cushion curves. Packaging Technology and Science 3:189-194.

Burgess, G. 1994. Generation of cushion curves from one shock pulse. Packaging Technology and Science 7: 169-173.

Campbell, A. C. 2010. The use of A-flute, B-flute, AC-flute and BC-flute corrugated paperboard as a cushioning material (Master of Science, Clemson University).

DataFit v7.1, Oakdale Engineering.

Daum, M. A. Simplified process for determining cushion curves - The stress-energy method. Proceedings from Dimensions 2006. San Antonio, TX (2006).

Guo, Y. F., W. Xu, Y. Fu and W. Zhang. 2010. Comparison studies on dynamic packaging properties of corrugated paperboard pads. Engineering 2:378-386.

Guo, Y. F. and J. H. Zhang. 2004. Shock absorbing characteristics and vibration transmissibility of honey-comb paperboard. Shock and Vibration 11:521-531.

Guo, Y. F., W. Xu, Y. Fu and H. Wang. 2011. Dynamic shock cushioning characteristics and vibration transmissibility of X-PLY corrugated paperboard. Shock and Vibration 18:525-535.

Kim, J. N., J. M. Sim, M. J. Park, G. S. Kim, J. S. Kim and J. M. Park. 2013. Analysis and Modelling of Vibration Performance for Multi-layered Corrugated Structure. J. of Biosystems Eng. 38(4):327-334.

KS M ISO 12192:2014. Paper and board - determination of compressive strength - ring crush method.

Marcondes, J. 1992. Cushioning properties of corrugated fiberboard and the effects of moisture content. Trans-actions of the ASAE 35(6):1949-1953.

Marcondes, J. K. Hatton, J. Graham and H. Schueneman. 2003. Effect of temperature on the cushioning properties of some foamed plastic materials. Packaging Technology and Science 16: 69-76.

Marcondes, P. Minimum sample size needed to construct cushion curves based on the stress energy method (Master of Science, Clemson University) (2010).

MIL-HDBK-304C : Package cushioning design.

Park, J. M. and J. G. Han. 2011. Transport packaging design engineering. Moonundang.

Navarro-Javierre, P., M. Garcia-Romeu-Martinez, V. Coloquell-Ballester and E. de-la-Cruz-Navarro. 2012. Evaluation of two simplified methods for determining cushion curves of closed cell foams. Packaging Technology and Science 25:217-231.

Potter, G.A. Performance of expanded polymer cushion materials at less than one inch in thickness. (Master of Science, Clemson University) (2010).

Sek M. and J. Kirkpatrick. 1997. Prediction of cushioning properties of corrugated fibreboard from static and quasi-dynamic compression data. Packaging Technology and Science 10:87-94.

Sek M., M. Minett, V. Rouillard and B. Bruscella. 2000. A new method for determination of cushion curves. Packaging Technology and Science 13:249-255.

Singh J, L. Ignatova, E. Olsen and P. Sighn. 2010. Evaluation of stress-energy methodology to predict transmitted shock through expanded foam cushion. Journal of Testing and Evaluation 38(6):1-7.

Wang, D. M. 2009. Cushioning properties of multi-layer corrugated sandwich structures. Journal of Sandwich Structures and Materials 1(11):57-66.

Wang, D. M., H. Gong and Z. Bai. 2013. Effect investigation of relative humidity and temperature on multi-layer corrugated sandwich structures. Journal of Sandwich Structures and Materials 15:156-167.